Published by IOP Publishing for Sissa Medialab

Received: *May 20, 2025*
Accepted: *July 3, 2025*
Published: *August 27, 2025*

20th Anniversary Trento Workshop on Advanced Silicon Radiation Detectors
Trento, Italy
4–6 February 2025

Performance of irradiated TI-LGADs at 120 GeV SPS pion beams

I. Velkovska,[a,*] **J. Duarte Campderrós**,[b] **M. Fernandez Garcia**,[b] **C. Gemme**,[c] **V. Gkougkousis**,[d] **A. Hennessy**,[d] **B. Hiti**,[a] **G. Kramberger**,[a] **R. López Ruiz**,[b] **A. Macchiolo**,[d] **N. Moffat**,[e] **E. Navarrete**,[b] **P. Rezaei Mianroodi**,[d] **E. Robutti**,[c] **M. Senger**[d] **and I. Vila**[b]

[a] *Jožef Stefan Institute,*
Jamova cesta 39, 1000 Ljubljana, Slovenia
[b] *Instituto de Física de Cantabria,*
Edificio Juan Jorda Avenida de los Castros s/n 39005, Santander, Spain
[c] *Istituto Nazionale Fisica Nucleare - Sezione di Genova (INFN),*
Via Dodecaneso 33, 16146, Genova GE, Italy
[d] *University of Zürich,*
Winterthurerstrasse 190, 8057 Zürich, Switzerland
[e] *Instituto de Microelectrónica (IMB) - Centro Nacional de Microelectrónica (CNM) - Consejo Superior de Investigaciones Científicas (CSIC), Carrer dels Til·lers, Campus UAB, 08193 Bellaterra, Barcelona, Spain*

E-mail: iskra.velkovska@cern.ch

Abstract: Trench-isolated (TI) LGADs, developed at FBK, are pixelated LGAD implementations where pads are separated by physical trenches etched within the silicon substrate and filled with a dielectric. Developed as an alternative approach to implant-based inter-pad separation (JTEs), this technology promises a dramatic reduction in inefficient regions, mitigating fill factor issues inherent to small-pitch pixelated LGAD matrices. Through a dedicated 120 GeV SPS pion test beam campaign, the time resolution, efficiency, and inter-pad distance of carbon infused irradiated TI-LGADs is presented for Minimum Ionizing Particles (MIP). Fluences up to 1.5×10^{15} n_{eq}/cm^2 are evaluated, for single trench implementations with varied trench width. The combined timing and tracking readout used in this study, integrating Region of Interest (ROI) triggering, sub-µm multi-object alignment, multi-channel waveform digitization and achieving a 5–7 µm spatial resolution through a MIMOSA26 telescope, are also reviewed. Preliminary results are discussed for temperatures of −25°C.

Keywords: Particle tracking detectors (Solid-state detectors); Radiation-hard detectors; Solid state detectors; Timing detectors

*Corresponding author.

https://doi.org/10.1088/1748-0221/20/08/C08023

2025 JINST 20 C08023

Contents

1 Introduction and motivation

The High Luminosity Large Hadron Collider (HL-LHC) aims to deliver an integrated luminosity of 3000 fb^{-1} between 2030 and 2041 [1], significantly enhancing its discovery potential. This increased luminosity will lead to a higher collision rate, resulting in greater event pileup within each bunch crossing.

ATLAS [2] and CMS [3] Phase-2 upgrades will implement timing detectors where the sensors may require a timing resolution in the range of 30–50 ps. Low-Gain Avalanche Detectors (LGADs) [4] are promising due to their internal gain and precision timing, but face fill factor limitations in pixelated designs due to field termination related structures at the inter-pad region, such as Junction Termination Extensions (JTEs).

Trench-Isolated (TI) LGADs [5] address such issues by using dielectric-filled trenches to isolate pads, improving the fill factor. Applications include possible replacements of the damaged High Granularity Timing Detector (HGTD) sensors during HL-LHC, outer disk layers in CMS/ATLAS Phase 3 [2, 3], and medical physics (e.g. proton-CT).

Carbon-infused trench-isolated LGAD (TI-LGAD) sensors were evaluated in test beams at CERN SPS (120 GeV pions) and DESY (4 GeV electrons). Time resolution, efficiency, and inter-pad performance of single-trench designs with varying trench widths were studied up to a fluence of 1.5×10^{15} n_{eq}/cm^2. Irradiation was done using 1 MeV neutron equivalent at the Jožef Stefan Institute's TRIGA reactor[1] [6, 7]. The setup featured ROI triggering with sub-micron alignment, CAEN DT5742 digitization [8] (500 MHz bandwidth, 5 GS/s), and 5–7 µm spatial tracking using a MIMOSA26 telescope. Measurements were performed at −25°C.

[1]Jožef Stefan Institute, Ljubljana, Slovenia.

2025 JINST 20 C08023

2 Characterized samples at the test beams

The R&D production of TI-LGAD (Trench-Isolated Low Gain Avalanche Diode) sensors by FBK[2] within the AIDAinnova WP6 project aimed to improve radiation hardness via carbon co-implantation in the gain layer. Variations in trench depth, width, and process were explored.

TI-LGADs address fill-factor limitations of standard LGADs, with the inter-pixel distance (IPD)—the no-gain region between adjacent gain areas — strongly affected by bias voltage and trench design.

The sensors, tested at SPS and DESY, have a 375 µm × 250 µm pixel pitch (figure 1a) and feature a single trench isolating adjacent pixels (figure 1b).

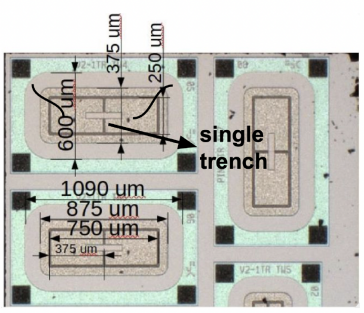

(a) Illustration of TI-LGAD device.

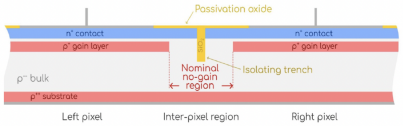

(b) Cross-sectional view showing the trench between pixels. Reproduced with permission from [9].

Figure 1. Single-trench TI-LGAD devices characterized in beam tests. Both channels are read out from the left and right pixels, with the inter-pixel trench forming a no-gain region.

For the beam tests reported, sensors from wafer 2 of the AIDAinnova production were used. These 45 µm thick sensors feature carbon implantation [10].

3 Test beam campaigns and experimental setup

TI-LGADs were tested at CERN SPS (120 GeV pions) and DESY (4 GeV electrons) using devices with different trench width (TW) parameters of the order of a few µm trench width: TW5 (unirradiated), TW4/TW6 (irradiated), and TW7 (PIN). Fluences of 0.8, 1.5, and 2.5×10^{15} n_{eq}/cm^2 were applied; results are shown only up to 1.5×10^{15} n_{eq}/cm^2 due to low signals in the PIN and at high fluence.

The efficiency results presented are for an unirradiated sample at 50 V and an irradiated sample (fluence of 1.5×10^{15} n_{eq}/cm^2) at 530 V.

While MIP time resolution can be studied with a beta source, it lacks precise position resolution and accurate efficiency measurement, unlike test beam setups with tracking systems for accurate trajectory reconstruction. The experimental setups for the February and October 2024 beam campaigns are shown in figure 2.

The CERN SPS H6 setup included: EUDET beam telescope [11] with MIMOSA26 sensors (18 µm pitch), Trigger Logic Unit [12], High and Low voltage sources, oscilloscope, CAEN digitizer [8] for read out of the DUTs, CROC 3D module with 25 µm × 100 µm pixels used for ROI selection,

[2]Fondazione Bruno Kessler, Trento, Italy.

2025 JINST 20 C08023

five DUTs, an HPK LGAD sensor with four pads used as time reference and piezoelectric actuators for DUT positioning [13].

The DESY setup was similar, with two movable DUT planes each equipped with Chubut2 boards [14] and one time reference detector, while a CROC 3D module with 50 µm × 50 µm pixels was used for defining the ROI.

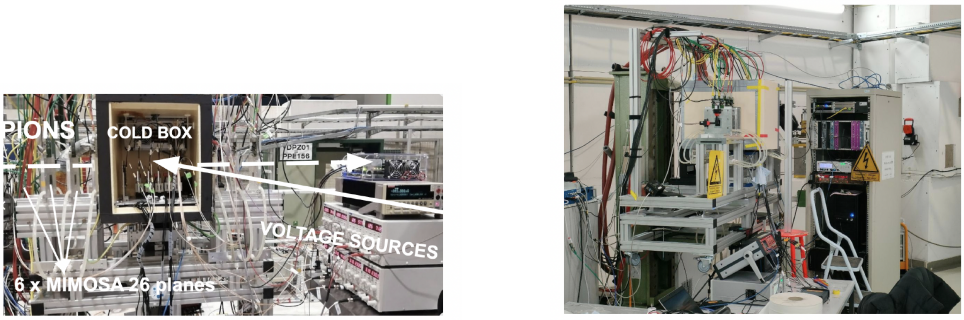

(a) SPS CERN, October 2024 (b) DESY, Hamburg, February 2024

Figure 2. Photographs of the test beam setups at SPS and DESY.

The DUTs were mounted on Chubut2 readout boards [15] (figure 3), each hosting two sensors with four wire-bonded channels per sensor. Each of the four on-board readout channels includes two amplification stages using PSA4-5043+ chips — ultra-low noise amplifiers (50–4000 MHz, 50 Ω matched), removing the need for external amplifiers.

Figure 3. Chubut2 readout boards [15] used to characterize TI-LGAD DUTs in beam tests.

4 Track reconstruction and integration of CMS ReadOut Chip

The CMS inner tracker ReadOut Chip was integrated into the tracking system, utilizing a 3D pixel sensor with a pixel pitch of 25 µm × 100 µm, as shown in figure 4. Figure 5 illustrates the distribution of track counts per bin used in the analysis, with an average of approximately 5.4 tracks per bin. The total number of reconstructed tracks is 49,000, and the DUT signals were split into two trigger groups using the CAEN 5742 16-channel digitizer based on the PSI DRS chip.

4.1 Triggering configuration

At the DESY test beam, a dedicated LGAD sensor provided the trigger. The DAQ rate, when the electron energy was set to 4 GeV, was approximately 3 Hz, recording around 100,000 events per run. CROC module was employed to reduce the background in the reconstruction thanks to its 25 ns time stamping, to be compared with the MIMOSA26 read-out time of 120 µs.

2025 JINST 20 C08023

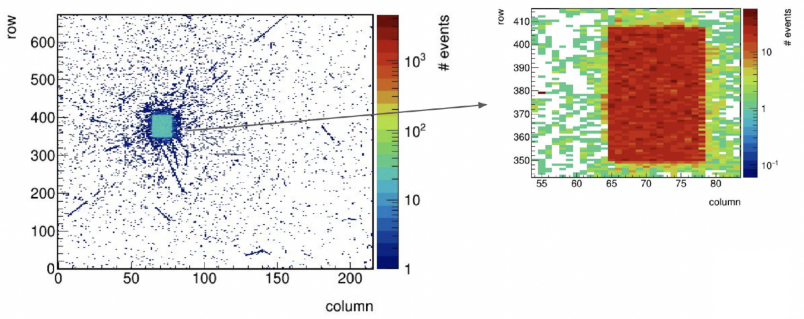

Figure 4. Left: Hitmap of the CROC with 49 000 reconstructed tracks with zoom on the ROI corresponding to the position of the HPK LGAD used as time reference.

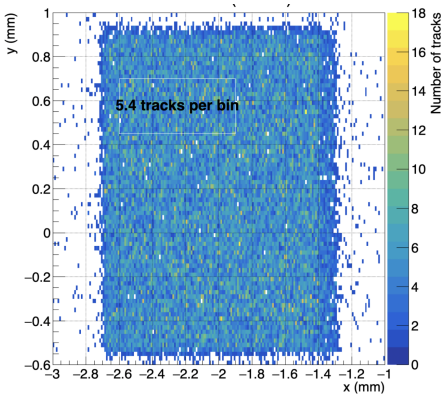

Figure 5. Reconstructed tracks in the PIN.

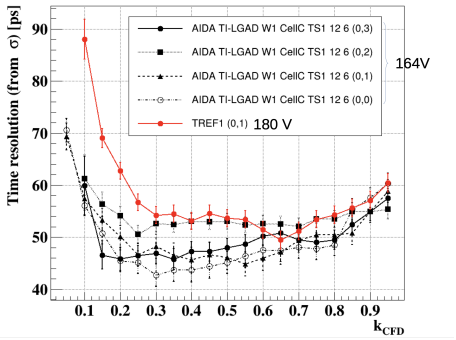

Figure 6. Time resolution for unirradiated DUTs.

In the October 2024 SPS test beam, the trigger combined the CROC HitOR signal with two downstream scintillators. This study focuses on the longest run, totaling 137,775 triggered events.

5 Results on time resolution of TI-LGADs (DESY test beam)

Time resolution at 4 GeV DESY test beam (without tracking) was evaluated using a three-stack method, where time differences between three objects are fitted with a Gaussian. The standard deviation (σ) of the fit represents the timing jitter. At a constant fraction discriminator (CFD) threshold of 40%, the extracted resolutions for the DUTs, and the timing reference (TREF) are approximately 44 ps, 48 ps, and 54 ps, respectively (figure 6).

Figure 7(a) shows a time resolution of 58 ps at DESY compared to 40 ps measured at SPS for a TI-LGAD irradiated to 1.5×10^{15} n_{eq}/cm^2, biased at 400 V and 530 V, respectively. In figure 7(b) are shown time resolutions at 50% CFD for unirradiated TI-LGADs biased at 164 V and irradiated to 1.5×10^{15} n_{eq}/cm^2 biased at 400 V. This underperformance may result from unoptimized electronics for low-capacitance devices, reference timing uncertainty, and peripheral pixel hits. The setup includes the DUT, a timing reference (TREF), and the trigger input to the CAEN digitizer. It should be noted that the measured time resolutions, may be influenced by the intrinsic jitter of the CAEN digitizer, which is measured not to be higher than approximately 20 ps [8].

2025 JINST 20 C08023

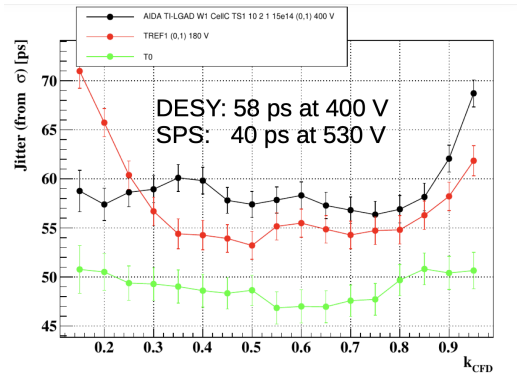

(a) Time resolution calculated through three-stack method, using DUT, timing reference (TREF), and a signal from trigger input

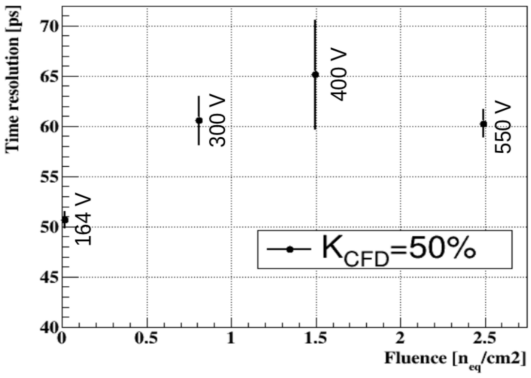

(b) Time resolutions at a constant fraction discriminator (CFD) threshold of 50% for all fluences

Figure 7. Time resolution results for TI-LGADs without tracking information.

6 Efficiency of the detector

Detection efficiency is the probability of registering a signal from an incident particle. In TI-LGADs, this is mainly limited by the fill factor and radiation damage. Trench isolation helps minimizing inactive regions between pixels, making spatial efficiency mapping essential. Radiation degrades gain with increasing fluence, lowering signal amplitude and potentially pushing signals below threshold.

6.1 Efficiency results

Efficiency was measured in the October 2024 SPS test beam using ~49,000 tracks over a 1×2 pixel area. Results for an unirradiated TI-LGAD (TW5, 50 V) and irradiated samples (TW4, TW6 at 1.5×10^{15} n_{eq}/cm^2, 530 V) are presented. All sensors shared a daughterboard with two wire-bonded channels. The focus is on the inter-pixel distance (IPD), the gap between gain regions (figure 8), where field non-uniformities impact efficiency, charge sharing, and spatial resolution. Understanding IPD response aids future LGAD pixel optimization.

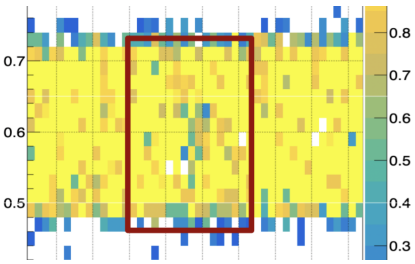

Figure 8. Efficiency map of an unirradiated TI-LGAD centered around the trench position in the inter-pixel area, highlighted by the red rectangle.

Figure 9 compares unirradiated and irradiated TI-LGADs with trench widths TW4 (narrowest), TW5, and TW6. Figure 9(a) shows the unirradiated sample, with an average efficiency of 95.3% ± 0.7% across two pixels (excluding periphery). Yellow marks full efficiency; blue indicates loss. Higher bias voltages are expected to enhance performance.

2025 JINST 20 C08023

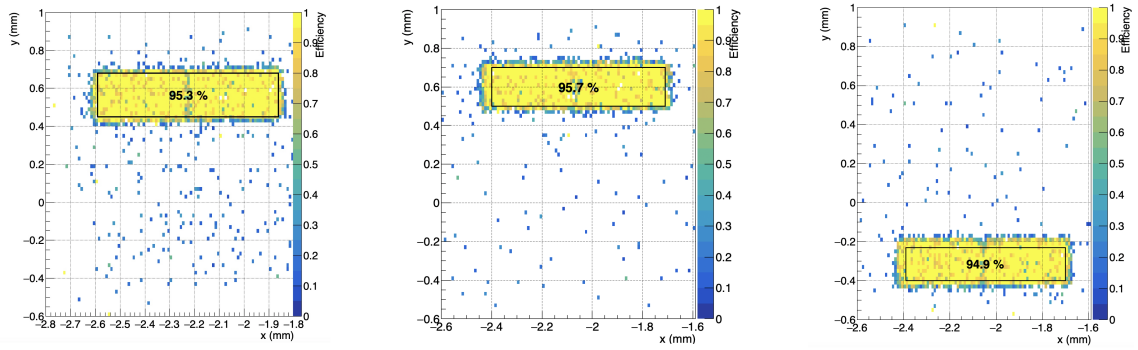

(a) Unirradiated TW5, 50 V. $S/N_{\text{peak}} = 48$, $S/N_{\text{cut}} = 13$

(b) Irradiated TW4, 530 V. $S/N_{\text{peak}} = 68$, $S/N_{\text{cut}} = 25$

(c) Irradiated TW6, 530 V. $S/N_{\text{peak}} = 68$, $S/N_{\text{cut}} = 25$

Figure 9. Efficiency maps for unirradiated and irradiated TI-LGAD samples.

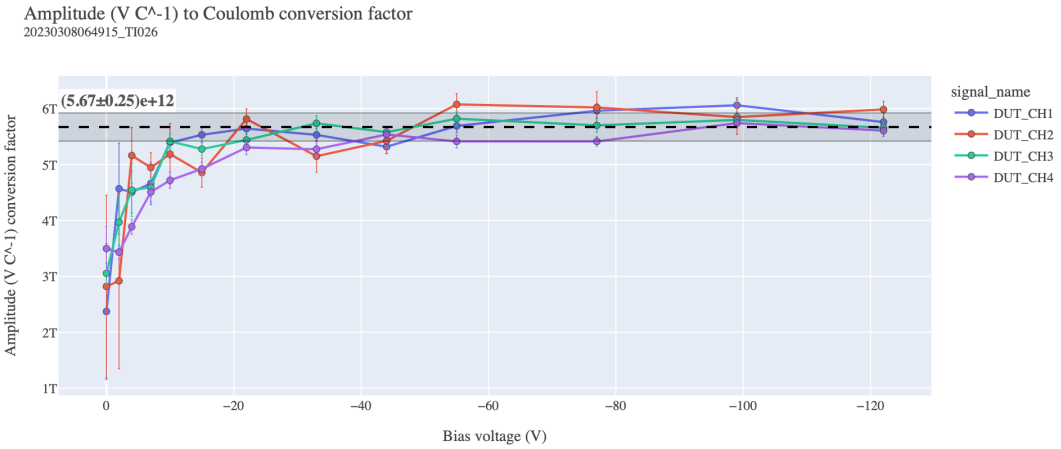

Figure 10. Measured amplitude to Coulomb conversion factor for different bias voltages and each of the four channels of the Chubut 2 board using a PIN diode from the TI-LGAD production. Reproduced with permission from [https://sengerm.github.io/Chubut_2/doc/testing/index.html#Figure:%20schematic%20of%20beta%20setup].

At 1.5×10^{15} n_{eq}/cm^2 biased at 530 V (figures 9(b), 9(c)), TW4 achieves $95.7\% \pm 0.8\%$ efficiency, comparable to TW6 at $94.9\% \pm 0.9\%$. Results are statistically consistent; systematic uncertainties (e.g., fluence variation, synchronization errors) are not included.

In our analysis, both the pulse height and the rising edge of the waveforms were used to evaluate the signals. Based on a measured system noise level of less than

$$V_{\text{noise,RMS}} < 1\,\text{mV},$$

and the Chubut 2 amplifier's conversion factor shown on figure 10 of

$$G = 5.67 \times 10^{12}\,\text{V/C} = 5.67\,\text{mV/fC},$$

the signal-to-noise thresholds used in the analysis ($S/N = 13$ for unirradiated and $S/N = 25$ for irradiated samples) correspond to charge thresholds of less than approximately

$$Q_{\text{thr,unirr}} < \frac{13 \times 1\,\text{mV}}{5.67\,\text{mV/fC}} \approx 2.3\,\text{fC}, \quad Q_{\text{thr,irr}} < \frac{25 \times 1\,\text{mV}}{5.67\,\text{mV/fC}} \approx 4.4\,\text{fC}.$$

2025 JINST 20 C08023

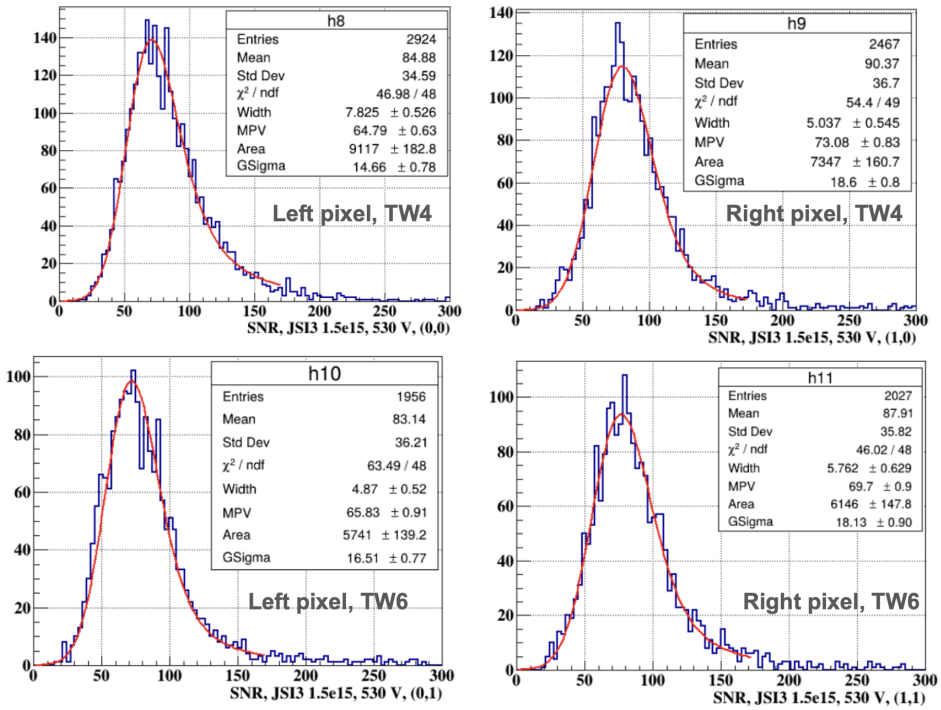

Figure 11. MPV for irradiated TI-LGADs at 1.5×10^{15} n_{eq}/cm^2 biased at 530 V.

The signal-to-noise ratio (S/N) distributions for the irradiated DUT at a fluence of 1.5×10^{15} n_{eq}/cm^2 and a bias voltage of 530 V are shown in figure 11. The most probable value (MPV) of the S/N is approximately 68. Assuming an average noise level of

$$V_{\text{noise,RMS}} \approx 0.8\,\text{mV},$$

this corresponds to a most probable signal amplitude of

$$V_{\text{signal,MPV}} = 68 \times 0.8\,\text{mV} = 54.4\,\text{mV},$$

and a most probable collected charge of

$$Q_{\text{MPV}} = \frac{54.4\,\text{mV}}{5.67\,\text{mV/fC}} \approx 9.6\,\text{fC}.$$

Assuming a 45 µm thick detector, a minimum ionizing particle deposits approximately

$$Q_{\text{MIP}} \approx 0.58\,\text{fC}$$

without gain. Therefore, the gain at 530 V for irradiated sample is

$$\text{Gain} = \frac{Q_{\text{MPV}}}{Q_{\text{MIP}}} \approx \frac{9.6\,\text{fC}}{0.58\,\text{fC}} \approx 16.6.$$

2025 JINST 20 C08023

6.2 Efficiency analysis

The analysis yielded a total of 321 tracks pointing inside the pixel region, all of which exhibited a signal amplitude above the predefined threshold, resulting in an observed pixel efficiency of approximately $\approx 100\%$. Notably, for one of the pixels in TW4 TI-LGAD, 5366 events were registered with a detected signal but without any corresponding track pointing to that pixel. This corresponds to a fraction of approximately 16.7% of signal-only events relative to efficient tracks, suggesting a significant number of potentially misreconstructed tracks or noise triggers. When merging channels of the two pixels together in the efficiency analysis, the total number of entries increased to 2343 about 2000 more than in the single-pixel analysis likely because some tracks are reconstructed by the neighboring pixel inside the pixel region under study and vice versa. This overlap causes signals to be attributed to adjacent pixels, contributing to the apparent signal-only events. These results indicate that the apparent inefficiency is not due to silicon sensor performance but is dominated by tracking reconstruction limitations. Further investigation is warranted to characterize the spatial distribution of these inefficient or misreconstructed tracks to conclusively separate tracking inefficiency from silicon inefficiency.

Efficiency projections along the X-axis for unirradiated (TW5) and irradiated (TW4) samples at a fluence of 1.5×10^{15} n_{eq}/cm^2 are shown in figure 12. These projections demonstrate only minor localized inefficiencies in the inter-pixel (IP) region. Devices with narrower trench widths operated at high bias voltages show improved efficiency, consistent with enhanced charge collection. The inter-pixel distance (IPD) measured has a value of 30 µm for the non-irradiated sensor (figure 12a) and 20 µm for the irradiated sensor (figure 12b).

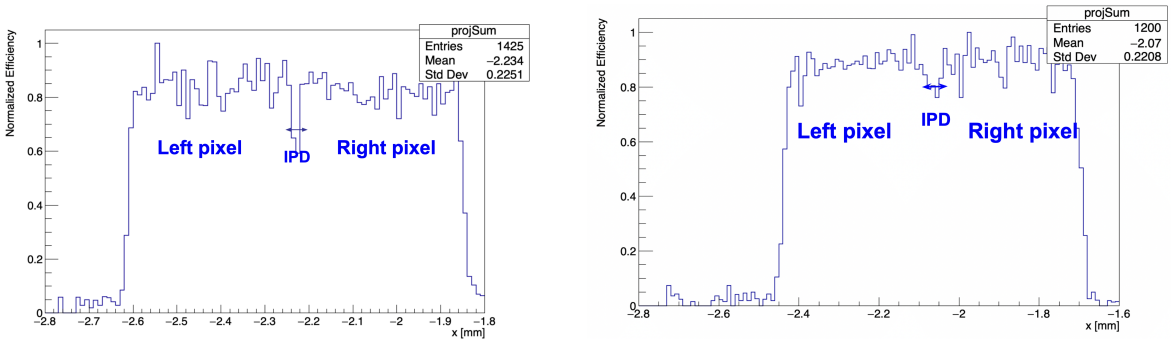

(a) X projection of unirradiated TI-LGAD (TW5)

(b) X projection of irradiated TI-LGAD (TW4)

Figure 12. Efficiency projections of TI-LGADs.

7 Conclusions

We presented results for both unirradiated and irradiated TI-LGADs, with fluences up to 1.5×10^{15} n_{eq}/cm^2. Irradiated devices show stable operation at 530 V, and time resolution improvements are expected with tracking. Efficiency measurements confirm that TI-LGADs maintain high efficiency at 530 V after irradiation.

2025 JINST 20 C08023

Acknowledgments

The authors acknowledge financial support from the European Union's Horizon 2020 Research and Innovation Programme under Grant Agreement No. 101004761. The authors also acknowledge the financial support from the Slovenian Research and Innovation Agency (ARIS P1-0135-27, J7-5 4419, PR-12843). This work was partially funded by Grant PID2023-148418NB-C41, funded by MCIN/AEI/10.13039/501100011033, and by the Complementary Plan in Astrophysics and High-Energy Physics (CA25944), project C17.I02.P02.S01.S03 CSIC, funded by the Next Generation EU funds, RRF and PRTR funds, and the Autonomous Community of Cantabria. Jordi Duarte Campderros acknowledges grant RYC2023-044327-I funded by MICIU/AEI/10.13039/501100011033 and by ESF+.

References

[1] I.B. Alonso et al., *High-Luminosity Large Hadron Collider (HL-LHC): Technical design report*, CERN-2020-010 (2020) [DOI:10.23731/CYRM-2020-0010].

[2] ATLAS collaboration, *Technical Design Report: A High-Granularity Timing Detector for the ATLAS Phase-II Upgrade*, CERN-LHCC-2020-007, CERN, Geneva (2020).

[3] CMS, collaboration, *A MIP Timing Detector for the CMS Phase-2 Upgrade*, CERN-LHCC-2019-003, CERN, Geneva (2019).

[4] G. Pellegrini et al., *Technology developments and first measurements of Low Gain Avalanche Detectors (LGAD) for high energy physics applications*, *Nucl. Instrum. Meth. A* **765** (2014) 12.

[5] M. Senger et al., *A Comprehensive Characterization of the TI-LGAD Technology*, *Sensors* **23** (2023) 6225.

[6] L. Snoj, G. Žerovnik and A. Trkov, *Computational analysis of irradiation facilities at the JSI TRIGA reactor*, *Appl. Radiat. Isot.* **70** (2012) 483.

[7] K. Ambrožič, G. Žerovnik and L. Snoj, *Computational analysis of the dose rates at JSI TRIGA reactor irradiation facilities*, *Appl. Radiat. Isot.* **130** (2017) 140.

[8] CAEN, *DT5742 - 16 Channel 12-bit 5 GS/s Digitizer*, https://www.caen.it/products/dt5742/.

[9] M. Senger, *Development of Precise Timing and Position Detectors Towards 4D Tracking*, Ph.D. Thesis, University of Zurich (2024) [DOI:10.5167/uzh-263142].

[10] G. Paternoster, *Development of LGADs and 3D detectors at FBK*, presentation at *VERTEX 2021*, https://indico.global/event/1721/contributions/30369/.

[11] H. Jansen et al., *Performance of the EUDET-type beam telescopes*, *EPJ Tech. Instrum.* **3** (2016) 7 [arXiv:1603.09669].

[12] A. C. Martyniuk et al., *A Trigger Logic Unit for test beam experiments*, EUDET-Memo-2009-04 (2009).

[13] E.-L. Gkougkousis, E. Lemos Cid and V. Coco, *Considerations on time resolution of neutron irradited single pixel 3D structures at fuences up to 1017 neq/cm2 using 120 GeV SPS pion beams*, *Nucl. Instrum. Meth. A* **1070** (2025) 170012 [arXiv:2403.00627].

[14] M.G. Senger, *Testing*, Chubut Project Documentation, https://sengerm.github.io/Chubut_2/doc/testing/index.html.

[15] Mini-Circuits, *PSA4-5043+ SMT Low Noise Amplifier*, https://www.minicircuits.com/WebStore/dashboard.html?model=PSA4-5043%2B&srsltid=AfmBOopiTj6DEZkQwCt6LML3Qj1sCCDseEI41X0SyfFyB1v2lsCdFo5c [accessed December 2023].

2025 JINST 20 C08023